ELSEVIER

NeuroImage

www.elsevier.com/locate/ynimg
NeuroImage xx (2006) xxx – xxx

In vivo neuropathology of the hippocampal formation in AD: A radial mapping MR-based study

G.B. Frisoni,[a,b,d,*] F. Sabattoli,[a] A.D. Lee,[c] R.A. Dutton,[c] A.W. Toga,[c] and P.M. Thompson[c]

[a]*LENITEM Laboratory of Epidemiology Neuroimaging and Telemedicine, IRCCS Centro S. Giovanni di Dio-FBF, Brescia, Italy*
[b]*Psychogeriatrics Unit, IRCCS Centro S. Giovanni di Dio-FBF, Brescia, Italy*
[c]*Laboratory of Neuro Imaging, Brain Mapping Division, Department of Neurology, UCLA School of Medicine, Los Angeles, CA 90095, USA*
[d]*AFaR Associazione Fatebenefratelli per la Ricerca, Rome, Italy*

Received 17 September 2005; revised 2 March 2006; accepted 7 March 2006

Early involvement of the hippocampal formation is the biological basis of the typical learning deficit in Alzheimer's disease (AD). However, the hippocampal formation is unevenly affected by AD pathology, deposits of plaques and tangles being particularly dense in the CA1 field and subiculum. The aim of the study was to locate in vivo the structural changes within the hippocampal formation in AD patients of mild to moderate severity. A group of 28 AD patients and 40 cognitively intact persons (age 74 ± 9 and 71 ± 7 years) underwent T1-weighted high-resolution MR scans. The hippocampal formation was isolated by manually tracing on 35 coronal slices the outlines of the hippocampus proper and subiculum after registration to a common stereotactic space. Group differences were assessed with algorithms developed ad hoc that make use of three-dimensional parametric surface mesh models. In AD patients, significant atrophic changes amounting to tissue loss of 20% or more were found in regions of the hippocampal formation corresponding to the CA1 field and part of the subiculum. Regions corresponding to the CA2–3 fields were remarkably spared. We conclude that the regions of the hippocampal formation that we found atrophic in AD patients are those known to be affected from pathological studies. This study supports the possibility of carrying out in vivo macroscopic neuropathology of the hippocampus with MR imaging in the neurodegenerative dementias.

Introduction

The hippocampus is the key structure in the development of Alzheimer's disease. It allows encoding of new information through incoming and outgoing pathways with relatively little redundancy such that lesions to strategic though restricted regions can isolate the hippocampal formation from connected cortical and subcortical structures. The main input to the hippocampal formation comes from the entorhinal cortex, and the major output arises from the subicular region. In AD, the entorhinal cortex, the CA1 field, and the subicular region are all heavily affected by cell loss, plaques, and tangles (Hyman et al., 1984; Van Hoesen and Hyman, 1990), thus giving rise to functional isolation of the hippocampal formation. On the contrary, the CA2 and CA3 fields are relatively spared (Hyman et al., 1984; Van Hoesen and Hyman, 1990).

A number of studies have addressed tissue loss in the hippocampus with the use of MR imaging with a number of assessment tools ranging from visual rating scales to region-of-interest-based volumetry to computational neuronatomy methods (Ashburner et al., 2003; Frisoni et al., 2003). The vast majority have found hippocampal atrophy in AD patients when compared to elderly controls (Scheltens et al., 2002), but all have been unable to accurately localize where atrophy occurs in the hippocampus—except grossly in the head, body, and tail (Frisoni et al., 2002; Laakso et al., 2000a; Pitkanen et al., 1996).

Locating in vivo the structural changes in the hippocampal formation of patients with AD is of interest in that this might reflect pathological involvement and might allow to better investigate the biological basis of functional disruption. We applied a recently developed algorithm sensitive to local surface changes of closed structures–such as the hippocampal formation–to the segmented hippocampi of 28 patients with mild to moderate AD and compared them to 40 elderly controls in order to study the fine topography of the structural changes of the hippocampal formation.

Methods

Subjects

This study included 28 persons with mild to moderate probable AD (McKhann et al., 1984) recruited among outpatients seen at the "Centro San Giovanni di Dio Fatebenefratelli–The National

* Corresponding author. IRCCS Centro S. Giovanni di Dio-FBF, via Pilastroni 4, 25125, Brescia, Italy. Fax: +39 030 3501313/+39 030 3533 513.
E-mail address: gfrisoni@fatebenefratelli.it (G.B. Frisoni).
Available online on ScienceDirect (www.sciencedirect.com).

1053-8119/$ - see front matter © 2006 Elsevier Inc. All rights reserved.
doi:10.1016/j.neuroimage.2006.03.015

Center for Alzheimer's Disease", in Brescia, Italy–between November 2002 and January 2005. Disease severity was assessed with the Mini Mental State Examination (Magni et al., 1996), and only patients achieving a score of 12 or higher out of a maximum of 30 were included in the present study. History was taken with a structured interview from a knowledgeable informant (usually the patient's spouse) and was particularly focused on those symptoms that might help in the differential diagnosis of the dementias (hallucinations, gait, language, and behavioral disturbances) in order to avoid contamination of non-AD dementias in the study group. Laboratory examinations included complete blood count, chemistry profile, thyroid function, B12 and folic acid, and EKG. Structured neurologic examination (including primitive reflexes such as grasping, sucking, palmomental, and snout) was performed by a neurologist, and physical examination by a geriatrician. A comprehensive neuropsychological battery was administered including the trail making (Amodio et al., 2002), token (De Renzi and Vignolo, 1962; Spinnler and Rognoni, 1987), clock drawing (Shulman et al., 1993), letter and category fluency (Novelli et al., 1986), Rey auditory verbal learning (Carlesimo et al., 1996), Rey figure copy, and Rey figure delayed recall tests (Caffarra et al., 2002; Taylor, 1969). Behavior was assessed with the NeuroPsychiatric Inventory (Cummings et al., 1994) assessing delusions, hallucinations, agitation, depression, anxiety, euphoria, apathy, disinhibition, irritability, abnormal motor behavior, sleep disorders, eating disorders, and expanded to assess development and remittance of symptoms throughout the whole disease course.

Controls were 40 persons taken from an ongoing study of the structural features of normal aging (http://www.centroalzheimer.it/arcprog_eng.htm) whose age and gender composition was comparable to that of patients with dementia coming for observation in our hospital. This study recruits outpatients attending the Neuroradiology Unit of the "Città di Brescia" hospital, Brescia, aged 40 and older and undergoing brain MR scan for reasons other than cognitive impairment (usually headache and vertigo) whose scan is negative for major stroke, tumor, aneurysm, or other focal lesions (Riello et al., 2005). Incidental atrophy, white matter disease, and lacunes are not exclusionary criteria. Normality of cognitive functions is ascertained through the Mini Mental State Examination (Magni et al., 1996) and a structured interview. Twenty controls agreed to undergo neuropsychological testing. The clinical assessment and neuropsychological testing forms for patients and controls may be downloaded at: http://www.centroalzheimer.it/Prot%20Clin_esteso.doc and http://www.centroalzheimer.it/ProtNPS.BS.doc.

MRI scans

High-resolution MRI images were acquired on a Philips Gyroscan 1.0 T scanner. Three-dimensional (3D) T1-weighted sagittal images were acquired using fast field echo. The following acquisition parameters were used: TR 20 ms, TE 5 ms, flip angle 30°, field of view 220 mm, acquisition matrix 256 × 256, and contiguous 1.3 mm thick slices covering the entire brain.

Image processing

MR images were reoriented along the AC–PC line, voxels below the cerebellum were removed with MRIcro (www.psychology.nottingham.ac.uk/staff/cr1/mricro.html), the anterior commissure was manually set as the origin of the spatial coordinates for the normalization algorithm, and images were normalized by linear (12 parameter) transformation to a customized template using the Statistical Parametric Mapping (SPM99) software (www.fil.ion.ucl.ac.uk/spm). The hippocampi were manually traced on contiguous coronal brain sections by a single individual (FS) blind to diagnosis and following a standardized and validated protocol (Laakso et al., 1996). Hippocampi were delineated using an interactive software program developed at the LONI (Laboratory of NeuroImaging) at the University of California at Los Angeles (http://www.loni.ucla.edu/ICBM/ICBM_ResSoftware.html#seg3). Programs for performing the hippocampal surface analyses and visualizations are available to interested investigators by contacting one of the authors (PT). This program allows the user to make use of anatomical landmarks by viewing images in all three orthogonal planes simultaneously (Thompson et al., 2004a,b).

Tracings included the hippocampus proper, subiculum (subiculum proper and presubiculum), part of the fimbria where it cannot be discriminated from the body of the hippocampus, and the gyri of Retzius (CA1 field of the cornu Ammonis in the tail) (Fig. 1). Each hippocampus is comprised of approximately 30 to 40 consecutive slices, and tracing takes about 40 min for both hippocampi of each individual. An example of a full sequence of tracings can be found on http://www.centroalzheimer.it/public/ADHM2005.doc.

Normalized hippocampal volumes were obtained and retained for statistical analysis. Test–retest reliability was assessed by one of the authors (FS) on the hippocampal formation volumes of 10 patients and 10 controls assessed 3 days apart and gave good reliability figures (intraclass correlation coefficient = 0.88, 95% C.I. 0.73 to 0.95, for the right and 0.89, 95% C.I. 0.75 to 0.96, for the left hippocampus). This level of agreement is comparable to that obtained in prior studies (Laakso et al., 2000b; Pruessner et al., 2000).

White matter changes were assessed with the rating scale for age-related white matter changes (Wahlund et al., 2001).

Mapping radial atrophy

Three-dimensional parametric surface mesh models were generated from the manually segmented hippocampal tracings (Narr et al., 2004; Thompson et al., 2004a). These procedures allow measurements to be made at corresponding surface locations in each subject that may be compared statistically in 3D (Thompson et al., 1996). The 3D parametric mesh models of each individual's hippocampi were analyzed to estimate the regional specificity of hippocampal volume loss in AD compared to controls. To assess hippocampal morphology, a medial curve was automatically defined as the 3D curve traced out by the centroid of the hippocampal boundary in each image slice. The radial size of each hippocampus at each boundary point was assessed by automatically measuring the radial 3D distance from the surface points to the medial curve defined for individual's hippocampal surface model. Shorter radial distances were used as an index of atrophy (Thompson et al., 2004a).

Statistical maps and permutation testing

Atrophy maps were visualized on 3D models of the hippocampal formation where the dorsal and ventral surfaces can be appreciated indicating local group differences in radial hippocampal distance. Neuropathologic areas were mapped onto the models

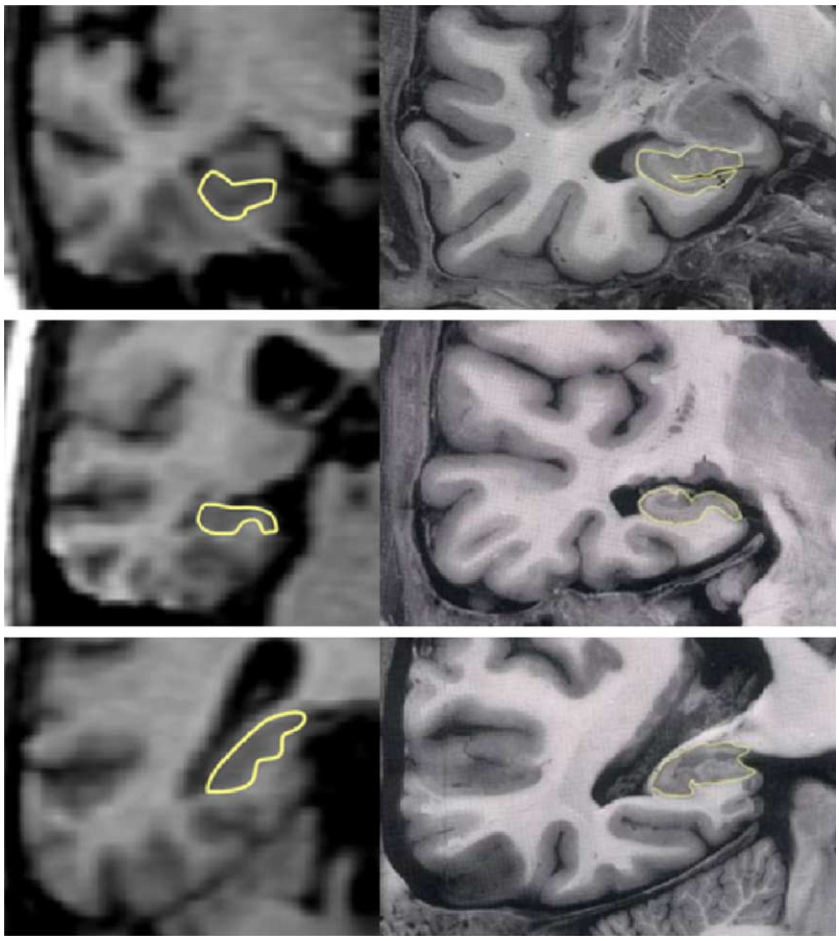

Fig. 1. Correspondence of the manual tracing of the hippocampal formation (left) to pathology (right). Selected slices are shown at the level of the head (upper), body (mid), and tail (lower row).

based on an atlas where these are shown together with the corresponding MR sections (Duvernoy, 1998) (Fig. 2A). The percent change relative to control and the associated *P* value describing the significance of group differences were plotted onto the model surface at each point of the hippocampus using a color code to produce statistical maps. Overall *P* values were computed for the maps of the left and right hippocampal formation using a permutation testing approach. Permutation methods measure the distribution of features in statistical maps that would be observed by accident if the subjects were randomly assigned to groups (Thompson et al., 2003) and provide a *P* value for the observed effects that is corrected for multiple comparisons.

Results

Table 1 shows that AD patients and control were similar in their sociodemographic features. The left and right hippocampal volumes in AD were 32% and 36% smaller than controls. Table 2 shows that the neuropsychological performance of patients was as expected for mild to moderate patients.

Fig. 2 shows that hippocampal volume loss in AD of 15% or greater (Fig. 2B) corresponded generally to a *P* value < 0.05 (Fig. 2C) and mapped mainly to regions corresponding to the CA1 sector and part of the subiculum (Fig. 2A). In the head of the hippocampus, the CA1 field is located on the superior, medial, and lateral aspects, in the body on the superior–lateral and inferior–lateral aspects, and in the tail virtually in all its aspects (Fig. 2A). These regions were atrophic in our AD patients except for the medial part of the dorsal surface of the head on both sides.

The CA2 and CA3 fields are located on the dorsal surface of the hippocampal formation in a strip stretching from medial to lateral between the most posterior head region and the most anterior tail region (Fig. 2A). The regions corresponding to the CA2–3 fields were relatively spared in our AD patients. Only one restricted patch of atrophy was present on both sides located on the superior–mesial aspect of the dorsal surface, just medial to the fimbria.

A large strip located on the medial and lateral part of the ventral surface of the body and tail and approximately corresponding to the presubicular and subicular regions was also spared. In the head, the ventral subicular region was more heavily affected than in the body and tail, mainly to the right. Patches where no atrophy was detected were present on both sides and located medially and laterally, in the region corresponding to the presubiculum.

The permutation test was highly significant ($P = 0.0001$ on both sides) indicating that the overall maps are very unlikely to have been obtained by chance.

Discussion

In this study, we mapped tissue loss in the hippocampal formation of patients with mild to moderate AD. We used a procedure based on manual tracing of the hippocampal boundaries and computer-assisted mathematical post-processing that reveals tissue loss occurring on the hippocampal surface, e.g., in regions corresponding to the CA1–3 fields and subiculum/presubiculum.

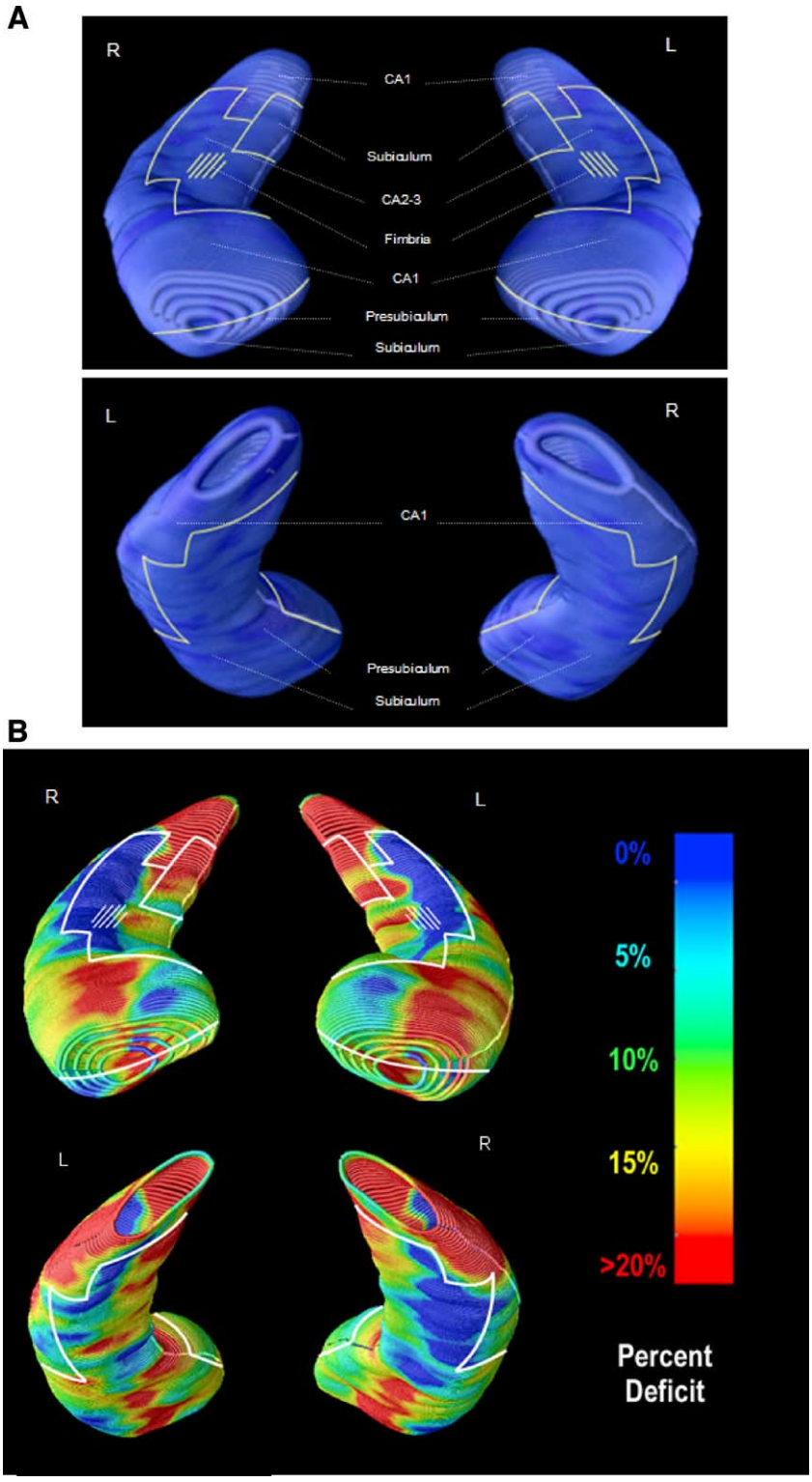

Fig. 2. (A) Topographic correspondence of pathology on blank MR-based models of the hippocampal formation of normal controls. Based on Duvernoy (1998), where neuropathologic areas are shown in 7 equally spaced coronal slices spanning the entire length of the hippocampus. CA: cornu Ammonis. (B and C) Topographic distribution of atrophy in the hippocampal formation of 28 patients with Alzheimer's disease compared to 40 elderly controls.

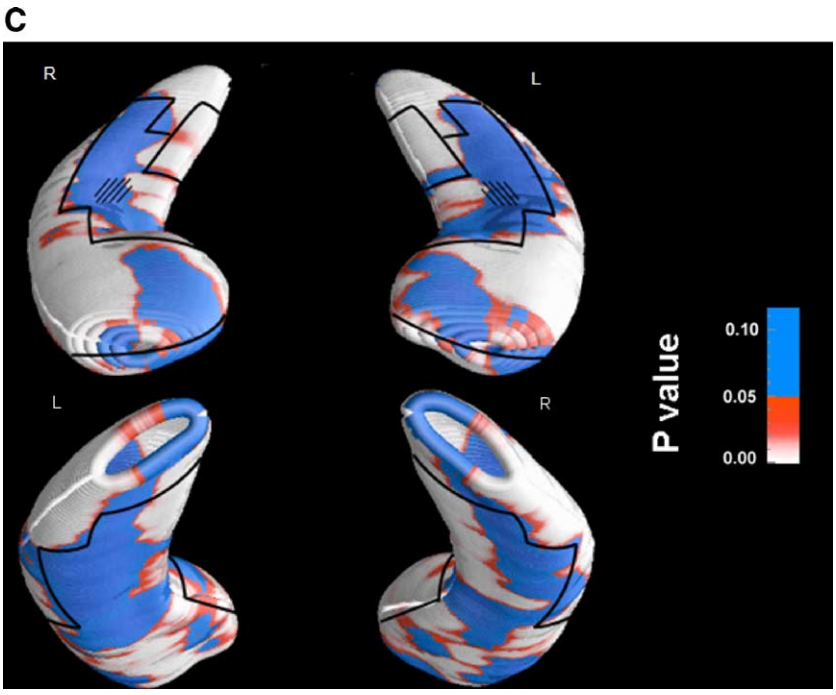

Fig. 2 (*continued*).

The procedure was able to visualize the profile of atrophy in regions corresponding to the CA1 fields and part of the subiculum/presubiculum and has shown that those corresponding to the CA2–3 fields were not significantly atrophic. This atrophy distribution largely corresponds to the known selective involvement of hippocampal regions by AD pathology.

Hippocampal afferents from association cortices converge on the entorhinal cortex and, via the perforant pathway, project to the dentate gyrus (Van Hoesen and Hyman, 1990). A set of intrinsic connections proceeds from the dentate gyrus to the CA3 field and hence to the CA1 field (Van Hoesen and Hyman, 1990). The major efferent connections of the hippocampal formation to the cortex arise from the pyramidal cells of the CA1 field and project directly or via the subiculum to the cortex (Van Hoesen and Hyman, 1990).

Table 1
Sociodemographic and clinical features of patients and control subjects

		AD (n = 28)	Controls (n = 40)	P
Age		73.8 ± 9.4 [53.9–90.7]	71.2 ± 6.8 [55.7–85.5]	n.s.
Sex, female		22 (79%)	28 (70%)	n.s.
Education, years		6.5 ± 4.7 [0–23]	8.5 ± 5.1 [3–18]	n.s.
Disease duration, months		42 ± 20 [12–96]	–	–
MMSE		20.0 ± 3.8 [12–28]	–	–
Hippocampal volume (mm^3)	L	2728 ± 590 [1632–4390]	3521 ± 480 [2425–4664]	<0.0005
	R	2580 ± 570 [1360–3621]	3497 ± 568 [1341–4150]	<0.0005
White matter changes		4.5 ± 4.4 [0–17]	3.7 ± 4.3 [0–18]	n.s.

Figures denote means ± SD [range]. P denotes significance on t test or χ^2.
MMSE: Mini Mental State Examination.
White matter changes were assessed with the rating scale for age-related white matter changes. Hippocampal volumes were normalized to the cranial size of a common template (see Methods), and volumes are therefore reported in cubic millimeters after normalization to the standard template.

Table 2
Neuropsychological features of patients and control subjects

	AD (n = 28)	Controls (n = 20)	P
Memory			
Rey's list immediate recall	18.0 ± 6.2 [3–32]	39.2 ± 8.8 [20–55]	<0.0005
Rey's list delayed recall	0.9 ± 1.6 [0–6]	9.1 ± 3.6 [3–15]	<0.0005
Visuospatial function			
Rey copy	13.0 ± 13.2 [0–36]	31.3 ± 6.3 [10–36]	<0.0005
Verbal fluency			
Letter	17.0 ± 8.9 [5–46]	30.0 ± 8.0 [17–50]	<0.0005
Category	15.5 ± 6.0 [5–30]	35.3 ± 8.3 [23–50]	<0.0005
Psychomotor speed			
Trail making test A	144 ± 72 [53–337]	49 ± 17 [28–87]	<0.0005
Executive functions			
Trail making test B–A	216 ± 132 [30–490]	86 ± 44 [24–178]	0.003
Comprehension			
Token test	27.5 ± 5.7 [17–36]	31.9 ± 3.0 [24–35]	0.005

Pathology affecting the CA1 field and subiculum in Alzheimer's disease results in the hippocampus becoming functionally disconnected from its target areas. The dentate gyrus, CA4, CA3, and CA2 fields are generally relatively spared by AD pathology.

The topographic distribution of the cornu Ammonis' fields, dentate gyrus, and subiculum is such that the CA1, CA2, and CA3 fields and subiculum lie on the surface of the hippocampal formation (Fig. 2A). On the contrary, the dentate gyrus is located in the central core, and the CA4 folds itself into the dentate gyrus such that they both lie distant from the surface. Thus, atrophy of the CA1, CA2, and CA3 fields and subiculum can be appreciated by our technique while atrophy of the CA4 field and dentate gyrus cannot be appreciated (only a tiny portion of the CA4 field is located on the dorsal surface of the tail of the hippocampus proper that can hardly be appreciated with the resolution of conventional MR scanners) (Duvernoy, 1998).

In our AD patients, we found atrophy in the hippocampal formation in regions corresponding to the CA1 field except for the medial part of the dorsal surface of the hippocampal head on both sides. We do not know why this area is relatively spared, although it may be hypothesized that it might be functionally connected to structures unaffected by the disease. Albeit small, the hippocampus is a highly differentiated structure. With an fMRI paradigm, Strange et al. (1999) provided evidence for functional segregation within the human hippocampus during learning by showing that the anterior hippocampus processes novel stimuli, whereas the posterior hippocampus processes familiar stimuli. Zeineh et al. (2003) have found that regions corresponding to the CA2–3 fields are activated during storage, while those corresponding to the subiculum to retrieval of newly learned information. Further studies will need to investigate the relationship between functional and structural changes of the hippocampus in patients with AD.

We found no sign of atrophy in the regions corresponding to CA2 and CA3 fields. This is in line with the notion that these are relatively spared by AD pathology (Van Hoesen and Hyman, 1990). The CA4 sector is also known to show generally relatively little AD pathology (Van Hoesen and Hyman, 1990), but it cannot be visualized conveniently in the present study due to its deep location inside the core of the hippocampal formation.

The interpretation of the findings in the subicular region is less straightforward. The subicular region is divided into four subregions from medial to lateral: parasubiculum (adjacent to the CA1 field), presubiculum, subiculum proper, and prosubiculum. All subregions are affected by AD pathology except the presubiculum and parasubiculum that are relatively spared (Van Hoesen and Hyman, 1990; Hyman et al., 1984). We found atrophy affecting most of the subicular region in the area of the head of the hippocampus and less widespread atrophy in the body and tail regions. It would be tempting to hypothesize that the non-atrophic regions correspond to the presubiculum and parasubiculum, but while this might be the case at most in the head (where patches unaffected by atrophy can be seen in a medial region that might roughly correspond to the presubiculum), this can hardly be the case elsewhere. Of course, the lack of correspondence between the present in vivo findings and pathological data in the literature might also be ascribed to imperfect localization of the subicular subregions in our material. Higher-resolution studies will be required to address the topographic distribution of atrophy and its functional meaning in the subicular area in AD.

Thompson et al. (2004a) used the same algorithms to map structural changes of the hippocampus and temporal horn at baseline and over a 2-year period in 12 patients with AD. Interestingly, they also have found that atrophy in the head of the hippocampus spared the medial dorsal region. However, the small sample size in that study may have limited the power to detect subtle atrophy in other hippocampal areas. Csernansky et al. (2000) used a related hippocampal surface modeling approach to map differences in 18 patients with Alzheimer's disease. In their approach, the 3D shape of the hippocampus is examined and can be averaged across subjects within a group, as in our study. They found atrophy mainly located on the lateral aspect of head, body, and tail, and to the dorsal and lateral surface of the head. Notably, this pattern is similar to that found in the present study. At variance with the present findings, however, in Csernansky et al.'s (2000) study, the medial aspect of the tail was spared and atrophy was relatively greater in the left hippocampus. Although the approaches agree on the major regions of atrophy in AD, the two methods may differ in their power to detect more subtle or diffuse atrophy, especially with small sample sizes.

Some caveats should be underlined. First, the use of hippocampal surface models relies on manual tracing, and systematic bias due to changes in the anatomy of the hippocampus of patients might adversely affect its reliability. In any given subject, there will be minor errors in assessing the distance between the central line threading down the center of the structure and the hippocampal surface. Some of the error derives from the resolution of the scanner, in that the voxel size is of the order of 1 mm. Other sources of error derive from the manual tracing method, although the reliability for the method has been shown to be high (Thompson et al., 2004a). If these errors in the estimation of the hippocampal boundary are random, the efforts of digitization error on the hippocampal shape should be substantially reduced (in proportion to the inverse square of the number of subjects when the surface models are averaged together). The technique will therefore pick up atrophy and should assess it accurately, even if the manual tracing does not consistently hit the actual boundary of a structure. However, it is possible that there is a systematic bias in these tracings that is correlated with diagnosis. Although the tracings are made by raters blind to diagnosis, any difference in image contrast between AD and healthy elderly subjects could, in principle, alter the boundary. These effects are likely to be minor, if present at all, as the major boundaries used are high contrast interfaces between CSF and gray or white matter; moreover, even a disease-related reduction in contrast would not necessarily imply a change in the position of the trace. In addition, any errors that are correlated with diagnosis would impair the absolute anatomical validity of the technique but would only serve to reinforce its clinical utility as they should err on the side of better differentiating patients from controls.

Second, the spatial resolution of the images we used is around 2 mm, and some neuroanatomical regions might be simply too small for the effect of AD pathology to be appreciated. Finally, the localization of neuroanatomical regions on our MR-based reconstructed model of the hippocampal formation is far from perfect due to interindividual variations of neuroanatomy and variability of image quality. In the future, more automated methods, once validated, might allow the study of local hippocampal changes in large groups of patients with AD, mild cognitive impairment, and other dementias.

Acknowledgments

Funding support for this work was provided in part by grants from the National Institute of Aging, National Institute for Biomedical Imaging and Bioengineering, and the National Center for Research Resources (P50 AG016570, R21 EB01651, R21 RR019771 to P.T., and P41 RR13642 and U54 GM072978 to A.W.T.).

References

Amodio, P., Wenin, H., Del Piccolo, F., et al., 2002. Variability of trail making test, symbol digit test and line trait test in normal people. A normative study taking into account age-dependent decline and sociobiological variables. Aging Clin. Exp. Res. 14, 117–131.

Ashburner, J., Csernansky, G., Davatzikos, C., Fox, N.C., Frisoni, G.B., Thompson, P.M., 2003. Computer-assisted imaging to assess brain structure in healthy and diseased brains. Lancet Neurol. 2, 79–88.

Caffarra, P., Vezzadini, G., Dieci, F., Zonato, F., Venneri, A., 2002. Rey–Osterrieth complex figure: normative values in an Italian population sample. Neurol. Sci. 22, 443–447.

Carlesimo, G.A., Caltagirone, C., Gainotti, G., 1996. The Mental Deterioration Battery: normative data, diagnostic reliability and qualitative analyses of cognitive impairment. The Group for the Standardization of the Mental Deterioration Battery. Eur. Neurol. 36, 378–384.

Csernansky, J.G., Wang, L., Joshi, S., et al., 2000. Early DAT is distinguished from aging by high-dimensional mapping of the hippocampus. Dementia of the Alzheimer type. Neurology 55, 1636–1643.

Cummings, J.L., Mega, M., Gray, K., et al., 1994. The Neuropsychiatric Inventory: comprehensive assessment of psychopathology in dementia. Neurology 44, 2308–2314.

De Renzi, E., Vignolo, L.A., 1962. The token test: a sensitive test to detect receptive disturbances in aphasia. Brain 85, 665–678.

Duvernoy, H.M., 1998. The Human Hippocampus. Functional Anatomy, Vascularization and Serial Sections with MRI, 3rd ed. Springer, Berlin.

Frisoni, G.B., Testa, C., Zorzan, A., et al., 2002. Detection of grey matter loss in mild Alzheimer's disease with voxel based morphometry. J. Neurol. Neurosurg. Psychiatry 73, 657–664.

Frisoni, G.B., Scheltens, P., Galluzzi, S., et al., 2003. Neuroimaging tools to rate regional atrophy, subcortical cerebrovascular disease, and regional cerebral blood flow and metabolism: consensus paper of the EADC. J. Neurol. Neurosurg. Psychiatry 74, 1371–1381.

Hyman, B.T., Van Horsen, G.W., Damasio, A.R., Barnes, C.L., 1984. Alzheimer's disease: cell-specific pathology isolates the hippocampal formation. Science 225, 1168–1170.

Laakso, M.P., Partanen, K., Riekkinen Jr., P., et al., 1996. Hippocampal volumes in Alzheimer's disease, Parkinson's disease with and without dementia, and in vascular dementia: an MRI study. Neurology 46, 678–681.

Laakso, M.P., Frisoni, G.B., Kononen, M., et al., 2000a. Hippocampus and entorhinal cortex in frontotemporal dementia and Alzheimer's disease: a morphometric MRI study. Biol. Psychiatry 47, 1056–1063.

Laakso, M.P., Hallikainen, M., Hanninen, T., Partanen, K., Soininen, H., 2000b. Diagnosis of Alzheimer's disease: MRI of the hippocampus vs delayed recall. Neuropsychologia 38, 579–584.

Magni, E., Binetti, G., Bianchetti, A., Rozzini, R., Trabucchi, M., 1996. Mini-Mental state examination: a Normative Study in an Italian elderly population. Eur. J. Neurol. 3, 198–202.

McKhann, G., Drachman, D., Folstein, M., Katzman, R., Price, D., Stadlan, E.M., 1984. Clinical diagnosis of Alzheimer's disease: report of the NINCDS-ADRDA Work Group under the auspices of Department of Health and Human Services Task Force on Alzheimer's Disease. Neurology 34, 939–944.

Narr, K.L., Thompson, P.M., Szeszko, P., et al., 2004. Regional specificity of hippocampal volume reductions in first-episode schizophrenia. NeuroImage 21, 1563–1575.

Novelli, G., Papagno, C., Capitani, E., Laiacona, M., Vallar, G., Cappa, S.F., 1986. Tre test clinici di ricerca e produzione lessicale. Taratura su soggetti normali. Arch. Psicol. Neurol. Psichiatr. 47, 477–505.

Pitkanen, A., Laakso, M., Kalviainen, R., et al., 1996. Severity of hippocampal atrophy correlates with the prolongation of MRI T2 relaxation time in temporal lobe epilepsy but not in Alzheimer's disease. Neurology 46, 1724–1730.

Pruessner, J.C., Li, L.M., Serles, W., et al., 2000. Volumetry of hippocampus and amygdala with high-resolution MRI and three-dimensional analysis software: minimizing the discrepancies between laboratories. Cereb. Cortex 10, 433–442.

Riello, R., Sabattoli, F., Beltramello, A., et al., 2005. Brain volumes in healthy adults aged 40 years and over: a voxel based morphometry study. Aging Clin. Exp. Res. 17, 329–336.

Scheltens, P., Fox, N., Barkhof, F., De Carli, C., 2002. Structural magnetic resonance imaging in the practical assessment of dementia: beyond exclusion. Lancet Neurol. 1, 13–21.

Shulman, K.I., Gold, D.P., Cohen, C.A., Zucchero, C.A., 1993. Clock-drawing and dementia in the community: a longitudinal study. Int. J. Geriatr. Psychiatry 8, 487–496.

Spinnler, H., Rognoni, G., 1987. Standardizazione e taratura italiana di test neuropsicologici. Ital. J. Neurol. Sci. 6 (Suppl 8).

Strange, B.A., Fletcher, P.C., Henson, R.N., Friston, K.J., Dolan, R.J., 1999. Segregating the functions of human hippocampus. Proc. Natl. Acad. Sci. U. S. A. 96, 4034–4039.

Taylor, L.B., 1969. Localisation of cerebral lesions by psychological testing. Clin. Neurosurg. 16, 269–287.

Thompson, P.M., Schwartz, C., Toga, A.W., 1996. High-resolution random mesh algorithms for creating a probabilistic 3D surface atlas of the human brain. NeuroImage 3, 19–34.

Thompson, P.M., Hayashi, K.M., de Zubicaray, G., et al., 2003. Dynamics of gray matter loss in Alzheimer's disease. J. Neurosci. 23, 994–1005.

Thompson, P.M., Hayashi, K.M., de Zubicaray, G.I., et al., 2004a. Mapping hippocampal and ventricular change in Alzheimer disease. NeuroImage 22, 1754–1766.

Thompson, P.M., Hayashi, K.M., Sowell, E.R., et al., 2004b. Mapping cortical change in Alzheimer's disease, brain development, and schizophrenia. NeuroImage 23 (Suppl 1), S2–S18.

Van Hoesen, G.W., Hyman, B.T., 1990. Hippocampal formation: anatomy and the patterns of pathology in Alzheimer's disease. Prog. Brain Res. 83, 445–457.

Wahlund, L.O., Barkhof, F., Fazekas, F., et al., 2001. A new rating scale for age-related white matter changes applicable to MRI and CT. Stroke 32, 1318–1322.

Zeineh, M.M., Engel, S.A., Thompson, P.M., Bookheimer, S.Y., 2003. Dynamics of the hippocampus during encoding and retrieval of face–name pairs. Science 299, 577–580.